PARAMETERS INFLUENCING FLOW-ACCELERATED CORROSION (FAC) IN THE SECONDARY SIDE OF NUCLEAR POWER PLANTS

By

M. Khatibi[1], D. H. Lister[1], A. Feicht[1], L. Liu[1], S. Uchida[2], K. Fujiwara[3], T. Ohira[4], H. Takiguchi[4], and K. Hisanume[4]

[1] Department of Chemical Engineering, University of New Brunswick, Canada

[2] Japan Atomic Energy Agency, Tokai, Japan

[3] Central Research Institute of the Electric Power Industry, Yokosuka, Japan

[4] Japan Atomic Power Co., Tokyo, Japan

Abstract

Thermal power plants have reported excessive pipe degradation because of Flow-Accelerated Corrosion (FAC) since the 1960s. Common features have been the use of carbon steel in regions of high flow rate and high turbulence with a water chemistry of modest alkalinity and free of oxidizing agents. It can be concluded that the main parameters that affect FAC are flow dynamics, water chemistry and composition of the materials used in pipework and components. A clear indication of FAC is the rapid wall thinning, usually in the presence of distinct flow-related markings, or scallops, on the surface. On more than one occasion, FAC has been responsible for large pipe failures that have led to serious damage and in some cases fatalities. After such a failure at the Mihama-3 PWR in 2004, a collaborative research program between Canada and Japan was initiated to improve the understanding of FAC by studying both the individual and the synergistic effects of feed-water system parameters. In an experimental water loop, three test sections were installed in series. Test section 1 contained probes made of the carbon steel of interest to measure on-line the FAC rate and electrochemical corrosion potential (ECP). Test sections 2 and 3 contained surface analysis probes for examination after removal via optical, SEM and Raman, techniques. The effects of flow and other parameters on FAC were studied using probes of different bore size, different material and several flow rates. Experiments were performed under neutral and ammoniated chemistries in de-oxygenated and oxygenated water. Threshold concentrations of oxygen to stifle FAC were determined. The individual and combined effects of system variables have now been determined in some detail and are presented here.

1. Introduction

Flow-Accelerated Corrosion (FAC) has caused deterioration of steel pipe-work and components in power plant feed-water and wet steam for many years. In more than one occasion FAC has been responsible for large pipe failures that have led to serious damage and in some cases fatalities. A recent accident which took place at the Mihama-3 PWR in August 2004 led to the death or serious injuriy of 11 workers. The rupture in the condensate piping was the result of excessive wall thinning caused by FAC (Figure-1). Common features in most secondary side accidents of nuclear power plants have been the use of carbon steel in locations of high coolant flow rate and high turbulence with alkaline water chemistry free of oxidizing agents. It appears that the main parameters that affect FAC are flow dynamics, water chemistry and composition of the materials used in pipework and components. The obvious indication of FAC is the wall thinning in the presence of clear flow-related markings, or scallops, on the surface.

Fig.1 Ruptured Pipe at Mihama-3 [1]

The Mihama-3 PWR had its 54 cm diameter feed-water piping operating at a temperature of about 142°C and pressure of 0.93 MPa with a coolant velocity of about 2.2 m/s. The pH of the coolant was 8.6 – 9.3 with a dissolved oxygen concentration of less than 5 ppb (parts per billion). [2]

To anticipate the accelerated thinning caused by FAC, a detailed model is required. Some data from previous studies are available to describe the effect of several separate parameters individually on FAC rate; however, information on the synergistic effects caused by combinations of several parameters is still required. Determining such multi-variable effects is the major objective of this research. Among the parameters which affect FAC, the focus of this research has mainly been on flow velocity, water chemistry, material composition and coolant

oxygen content. The determination of a threshold oxygen concentration necessary for stifling corrosion has been key.

To understand more thoroughly the mechanisms behind FAC in feed-water systems so that mitigating procedures can be formulated, the University of New Brunswick (UNB) and the Central Research Institute of the Electric Power Industry (CRIEPI) established the Canada and Japan Collaboration Research Program on the Fundamental Study of Flow-Accelerated Corrosion. [3]

The experimental procedures, test runs, and results will be presented in the following sections.

2. Experimental

2.1. Apparatus

The experimental loop at UNB is a pressurized, once-through system working at 150 psi and 140°C (see Figure 2). Water with the desired chemistry in a stainless steel tank of 120 L is pumped through a positive displacement pump of maximum capacity 6 L/min. It enters the main Hastelloy C-276 heater after passing through the interchanger and preheater, both made of stainless steel. Coolant with the desired temperature enters a series of test sections before leaving the high pressure part of the loop. After being cooled to room temperature, the coolant passes through a filter and an ion-exchange column and returns to the tank, whence it is recirculated through the loop. All the connecting tubing is made of stainless steel.

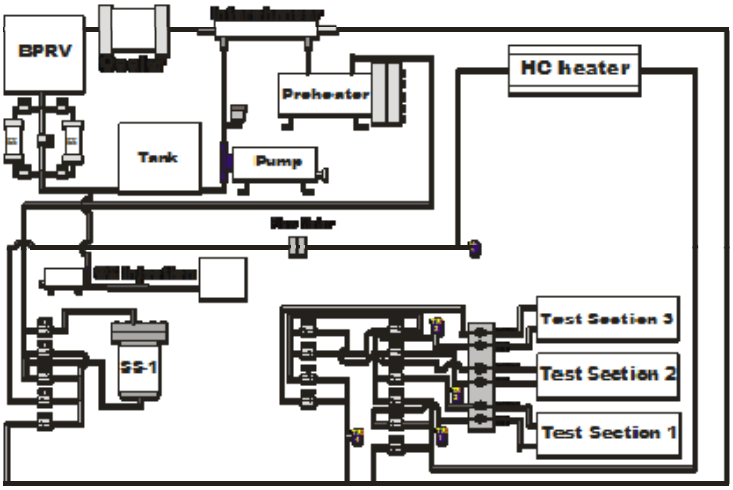

Fig.2 Schematic diagram of FAC loop at UNB

Three test sections were installed in series for these experiments. Test section one (TS1) contained resistance probes made of the material of interest, used to measure the FAC rate and electrochemical potential (ECP), and stainless steel probes for measurement of ECP and oxygen concentration (from ECP calibration curves). Probe inside diameters were 1.6 mm, 2.4 mm, and 3.2 mm and a continuous measurement of electrical resistance during a run indicated reduction in wall thickness and hence FAC rate. The test materials used were A-106B in the first run and STPT 480 for the rest. Their compositions as measured via chemical and other techniques are given in Table-1.

Table 1. Composition of carbon steel in experimental program (wt% - balance Fe)

	C	Si	Mn	P	S	Cr	Mo
A106 Grade B	0.2	0.31	0.62	0.020	0.012	0.019	0.004
STPT 480	0.25	0.24	0.80	0.017	0.010	0.001	<0.01

Test sections 2 and 3 (TS2, TS3) contained surface analysis probes for examination via SEM and Raman microscopy upon removal.

Figure 3 shows the typical configuration of probes for RUN-1.

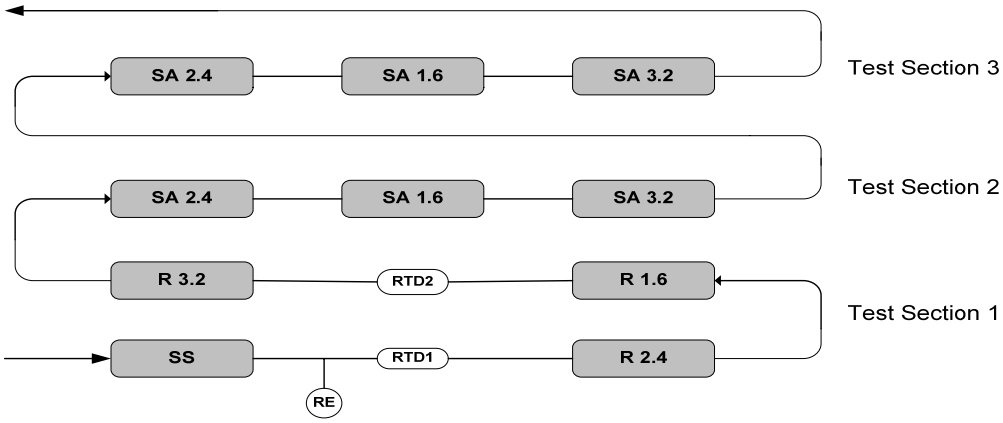

Fig.3 Test sections configuration for RUN-1

The controlling wall thickness of a resistance probe between the silver wires, which is over a length of 12.7 mm, was machined from about 2.0 mm to about 0.8 mm to raise electrical

resistance that could be measured accurately with a measurement system composed of a Keithley source meter, digital multimeter and switch system. The multimeter also served to measure electrochemical corrosion potential (ECP) relative to a reference electrode. Conax fittings employing lava pressure seals were used for resistance probes. The probes were electrically isolated along the sealing surfaces with Teflon heat-shrink and at the ends with Teflon spacers. To ensure the integrity of the probes under pressure a four-rod retaining cage was used to support each probe (see Figure 4). The rate of increase of resistance in probes, resulting from the increase in diameter by corrosion, gave a direct measure of FAC. Changes in resistance of 10 μΩ could be detected reliably. Resistance measurements were typically made at a frequency of one every 2-3 minutes. The resistivity of the CS A106 Grade B probe material and its variation with temperature were determined with a temperature-controlled furnace in separate measurements prior to the start of the experiments. Two RTDs to measure the temperature which is used for resistivity correction of the steel were installed as shown in Figure 3. [6]

Test Section 1 also contained one or two SS ECP probes of design similar to that of the 3.2 mm CS probes. A high-pressure Ag/AgCl electrode supplied by MPM Technologies was installed in TS1 as the reference. The reference electrode was adjacent to the first SS ECP probe and a bit farther from the other probes in TS1. The solution conductivity was low; however, distances from the reference electrode were short enough not to affect the trends in potential measurements which seemed consistent, though the absolute values may have been shifted slightly (see Figure 10 as an example of ECP measurements).

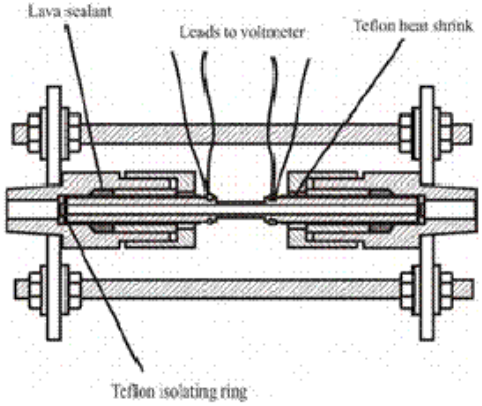

Fig.4 Resistance probe for on-line measurement of FAC rate and ECP

2.2. Experimental Runs

Table-2 presents the conditions in the experimental runs.

Table 2. Experimental runs

RUN	Material	Probe Diameter (mm)	Chemistry
1	SA-106 Grade B	2.4, 1.6, 3.2	Neutral, *[O_2]: ~0 ppb
2	STPT 480	2.4, 1.6	Neutral, [O_2]: 0 – 120 ppb
3	STPT 480	2.4, 1.6	pH 9.2 (NH_3), [O_2]: 0 – 10 ppb
4	STPT 480	2.4, 1.6	pH 10 (NH_3), [O_2]: 0 – 1 ppb
5	STPT 480	2.4, 1.6	pH 9.2 (NH_3), [N_2H_4]: 100 ppb, [O_2]: ~0 ppb

*[O_2]: Oxygen concentration

During these experiments the coolant was conditioned to simulate feed-water in pressurized water reactors (PWRs). Parameters variable in the loop were pH (controlled with ammonium hydroxide addition); pressure (maintained at the BPRV); flow rate (controlled by pump stroke adjustment); [O_2] (controlled by the injection of air-saturated water); conductivity (maintained with ion exchange resin); and temperature (controlled by heater output). Loop pressure (150 psig) and temperature (140^{o}C) were maintained constant. Except for RUN-1, in which the effect of flow rate and velocity on FAC rate was investigated, flow rate was maintained constant (1.63 LPM). In runs 2 – 4 the effect of oxygen concentration on FAC rate was determined at three pH values and a critical stifling concentration was determined for each. In RUN-5, the effect of hydrazine was investigated.

3. Results and Discussions

3.1. Commissioning Run (Neutral Water Chemistry)

A commissioning run was performed before RUN-1, using a stainless steel ECP probe, to check the ECP measurement with a varying oxygen concentration. The initial oxygen concentration was ~200 ppb and attained zero at the end. The pressure of the system was initially 500 psi and was reduced to 150 psi after few days. As shown in Figure 5, this pressure reduction led to a sudden drop in oxygen concentration, which can be explained by the partial sub-cooled boiling induced on the preheater surfaces and the resulting gas stripping. During this commissioning run the loop controllers were tuned and the purge gas was changed from H_2 to Ar (with no visible effect). Heater temperature was set to the value required for the experimental runs, ~140˚C, and flow rate was set on 1.63 L/min at the pump.

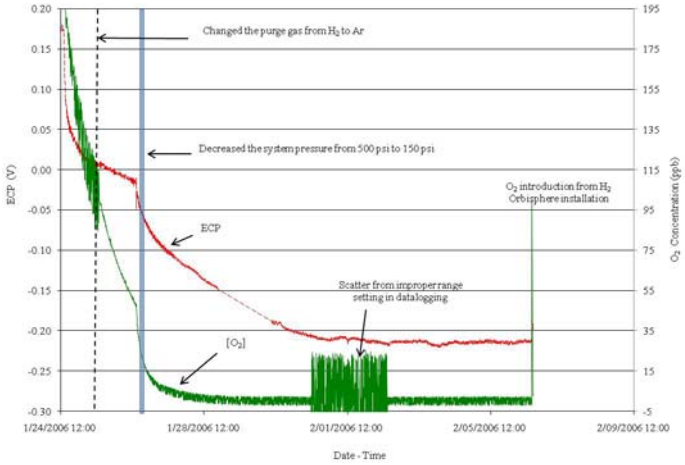

Fig.5 Commissioning Run – Neutral Water Chemistry

The ECP of the SS probe fell from ~0.175 V to ~ -0.220 V (SHE scale) during this commissioning run. It should be pointed out that there is a delay between the time that the ECP of the SS probe stabilized at its final value and the time that oxygen concentration reached its minimum.

3.2. RUN-1

Flow effects were studied in this run using three different diameter probes made of A106-B carbon steel. Coolant for this run was neutral water free of oxygen. Flow rates were varied to generate different linear velocities. The FAC rate during a given flow rate in Figure 6 was determined by taking the slope of the plot for the period of interest. Changes in slope reflect changes in FAC rate at the points of change in coolant flow rate.

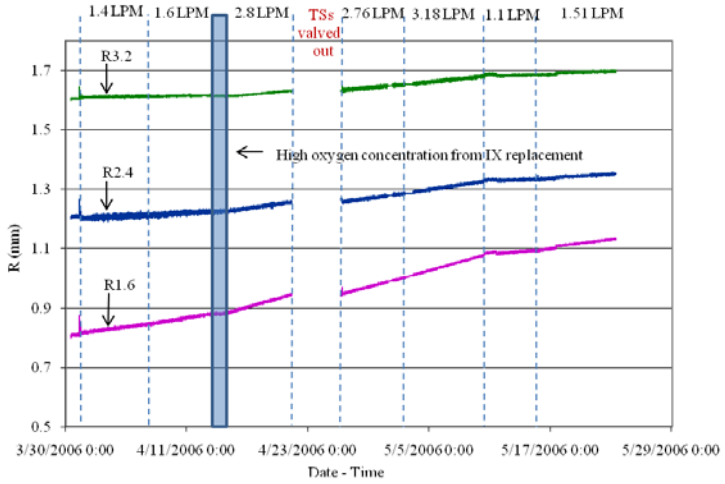

Fig.6 Probe radii – RUN-1 (Flow effects)

Power relationships, with respect to FAC rate, have been determined for linear velocity, Reynolds number, and shear stress using the experimental data, as shown in Table 3.

Table 3. Power Relationships – RUN-1

	R 1.6	R 2.4	R 3.2	FSFAC
Velocity	1.1738	1.8507	2.2466	1.5621
Re	1.3468	1.4555	1.8144	1.8030
Shear Stress	0.6087	1.0135	1.2463	0.8077

Surface analyses of probes from RUN-1 by SEM revealed scallop patterns. Probes that had seen higher velocity conditions presented smaller, more sharply-defined scallops at troughs and crests. The velocity was higher under higher flow rates and in smaller size probes (see Figure 7).

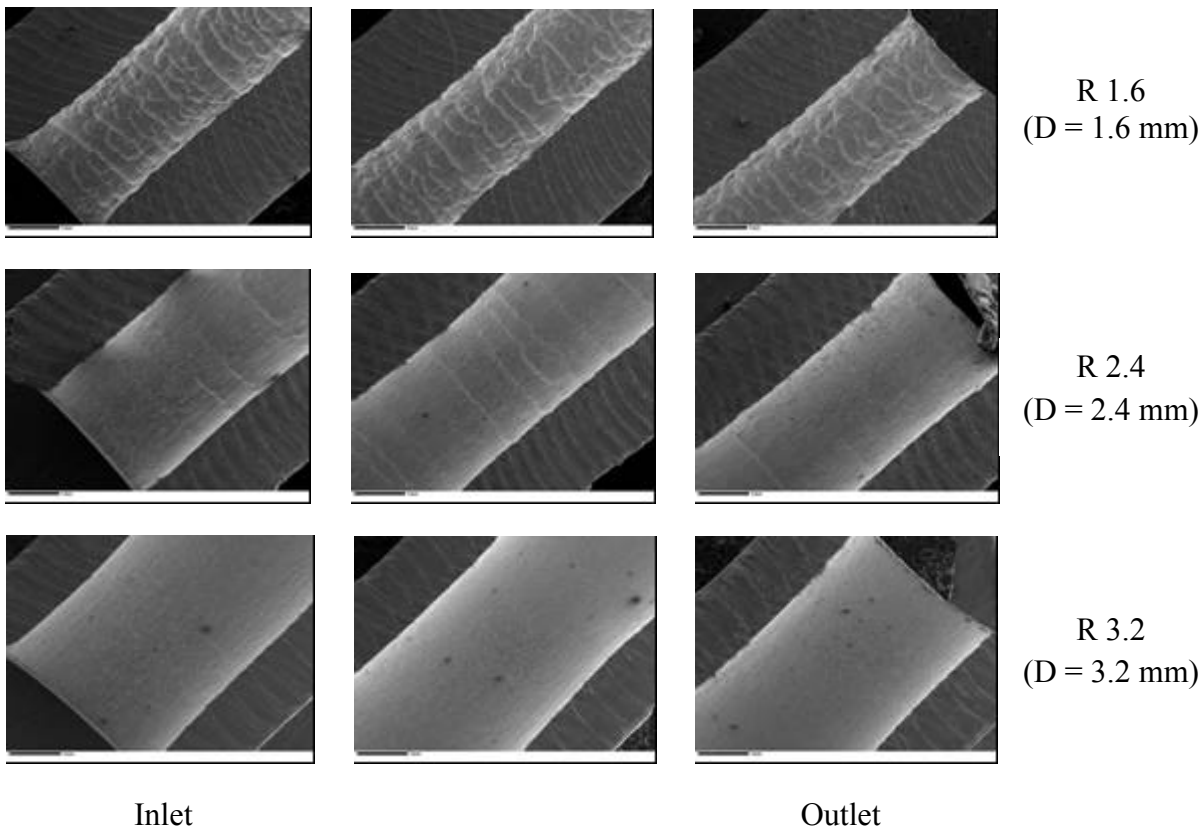

Fig.7 Surface analysis probes exposed to different flow rates at RUN-1

Examination of the surface showed the oxide as a double layer. The outer layer was more associated with scallop crests, while the inner layer was predominant in the troughs. EDX analysis showed that the oxide was quite thin - up to 1 μm thick. Figure 8a shows the oxide inner and outer layers formed on the 2.4 mm probe exposed to different flow rates. Table-4 presents the composition of the points indicated in Figure 8a. These revealed that there was a concentration of trace metals in the oxide formations. In particular, the Cr:Fe mass ratio varied from 3.35×10^{-3} in the crest oxide to 2.01×10^{-3} in the valley oxide; it was at a minimum in the base metal at 1.92×10^{-4} (see Table 1); note that EDX analysis on such thin oxides offers just an indication and not an accurate value due to interferences from the base metal. Since materials in the loop components do not release much, if any, Cr to the coolant, the Cr present in the oxide is assumed to be supplied from the base metal. This is a significant finding as Cr content of the oxide is the main contributor to its stability and corrosion resistance. Laser Raman analysis for all cases mainly revealed the characteristic peak for magnetite. Figure 8b shows the surface of the unexposed 2.4 mm probe.

a b

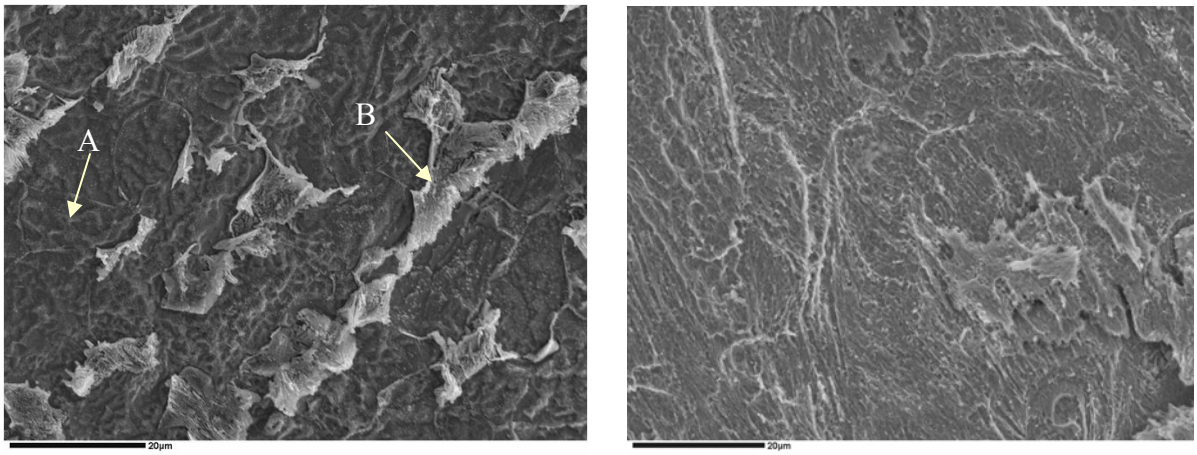

Fig.8 The surface of the 2.4 mm probe:

(a) After exposure to different flow rates (A: oxide valley, B: oxide crest) (b) Unexposed

Table 4. EDX analysis of crest and valley oxides on 2.4 mm probe exposed to different flow rates (%wt) - balance oxygen

	Si	Mo	Ti	Cr	Mn	Fe	Ni	Cu
Point A (Valley)	0.29	0.14	0.04	0.16	0.51	76.28	0	0.09
Point B (Crest)	0.52	0.46	0.07	0.25	1.13	74.54	0.35	0

3.3. RUN-2

Figure 9 presents FAC, as the change in probe radius, and oxygen concentration during the run. The initial FAC rate is zero because the two probes had been exposed to coolant containing oxygen for a few days before the period shown. The oxygen concentration dropped to zero in the first four days and then corrosion recommenced. Oxygen injection was then started at a low rate using a micrometer injection pump pumping air-saturated water to the loop upstream of the oxygen analyser Orbisphere. The oxygen concentration stabilized after a day or two allowing an increase in the injection flow rate. This trend continued until a point was reached where the corrosion stifled completely in the upstream probe (R2.4); the oxygen concentration corresponding to this point was measured at 38±3 ppb. The subsequent increase in oxygen concentration led to the stifling of the downstream probe (R1.6) a couple of hours later at an oxygen concentration of 44±6 ppb. Table 5 shows the injection rates and resultant FAC rate until stifling was reached. It may be noted that the FAC rates of both probes fell slightly as the $[O_2]$ was increased up to the stifling point mainly because of the rapid increase in probes diameters and therefore, the decrease of the coolant velocity as the result of FAC. This could also indicate an effect of oxygen on the oxide film. The stifling of the probes, however occurred very suddenly which therefore indicates that the interaction time required between the oxide and the bulk oxygen to achieve stifling was very short.

The injection pump was turned off to let the oxygen gradually decrease to zero, when corrosion recommenced in both probes. The test continued until the downstream probe (R 1.6), which had the smaller bore size, perforated.

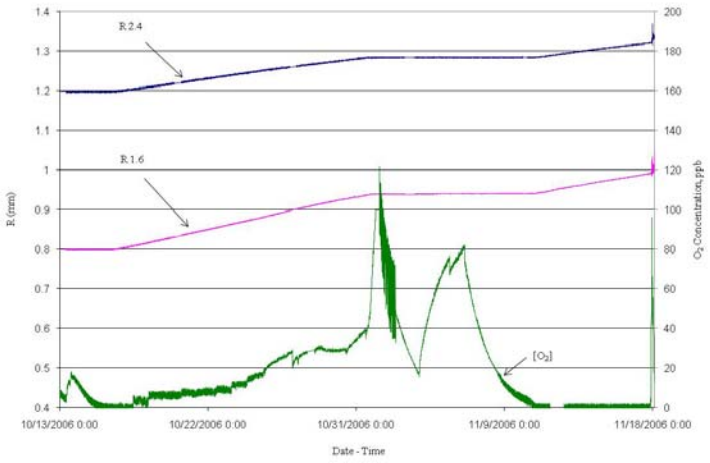

Fig.9 Probe radii – RUN-2 (Oxygen control by injecting air-saturated water)

As shown in Figure 10, the ECP varied roughly as the oxygen concentration, with the 2.4 mm probe showing the largest variation (between about -1 V vs. SHE at zero oxygen to about -0.17 V during the oxygen injection to 120 ppb).

Table 5. Oxygen injection and FAC rates (RUN-1)

Injection flow rate (mL/min)	$[O_2]$ (ppb)	FAC rate (R2.4) (mm/a)	FAC rate (R1.6) (mm/a)
1.61	3.46	2.00	3.17
2.01	6.54	2.23	3.36
2.31	7.82	2.23	3.23
2.51	9.34	2.23	3.43
3.02	12.03	2.15	3.36
3.42	15.84	2.12	3.50
3.82	29.45	2.00 – 1.86	3.43 – 3.21
4.02		1.71 - 0.0	2.59 - 0.0

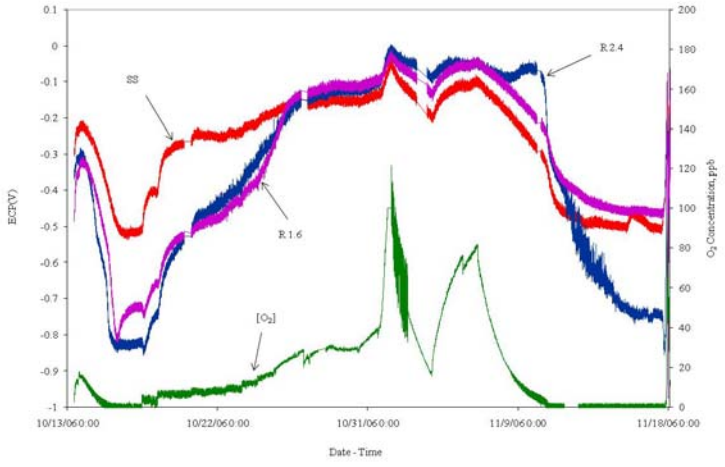

Fig.10 ECP - RUN-2 (Oxygen control by injecting air-saturated water)

SEM examination of surfaces of both probes indicated an absence of scallops, despite high FAC rates at the zero oxygen condition. The oxide patterns also seemed more random than those noted in RUN-1, which reflected the direction of flow. However, the same oxide features as those of RUN-1 were seen. Note that the surfaces analysed had seen oxygen concentrations up to only 20 ppb and no surfaces were examined following stifling. The oxides on the probes exposed to different [O_2] were predominantly magnetite, though laser Raman analysis revealed an increasing amount of hematite with increasing [O_2].

Comparison of results from RUN-2 with those from RUN-1 suggested that the lower Cr content of the probes in the former (by a factor of 1/19) was responsible for an increase in FAC rate (by a factor of ~2).

3.4. RUN-3

Following commissioning of the loop with ammoniated chemistry and associated ECP calibration, the 2.4 mm and 1.6 mm STPT 480 steel probes were exposed at nominally zero oxygen coolant under $pH_{25°C}$ of 9.2. The shift in magnetite solubility from ~119 ppb with pure water to ~14 ppb at $pH_{25°C}$ 9.2 [4] clearly raised the sensitivity of the system. Erratic spikes in [O_2] caused by loop manipulation, even though of the order of a few ppb, caused stifling of the probes. It is well known [5] that the threshold for stifling under ammoniated conditions is much lower than under neutral chemistry. Figure 11 shows the radius data during this period.

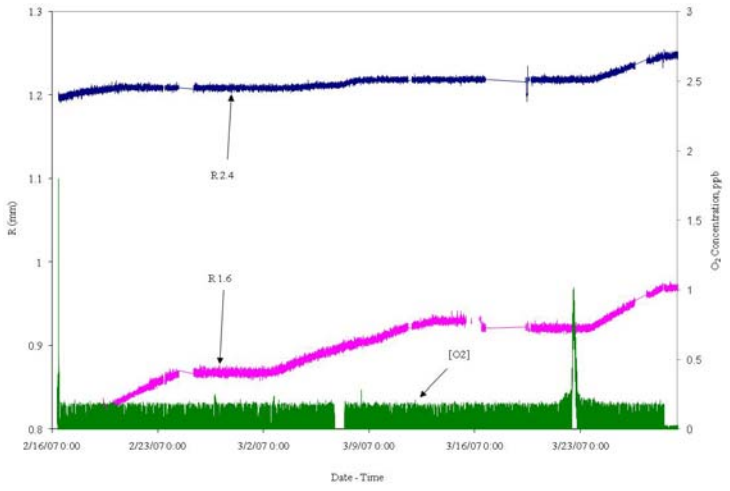

Fig. 11 Probe radii – RUN-3, first part

After the final stifling at low [O_2], the probes were replaced and the run was restarted. Upon examination of the 2.4 mm surface analysis probe, a thick hematite oxide film was discovered (see Figure 12) apparently progressing down the length of the probe. There was a distinct transition zone 1-2 mm in length, where the oxide changed in appearance from red to matt black and finally to the typical glossy black of FAC oxides. Laser Raman analysis confirmed the predominance of hematite upstream and magnetite downstream [2][6]. This front appears to be progressing down the length of the probe as a result of residual oxygen in the coolant. Presumably, oxygen concentration at the end of transition zone has been below the required level to form hematite. The rate at which this front progresses is unknown.

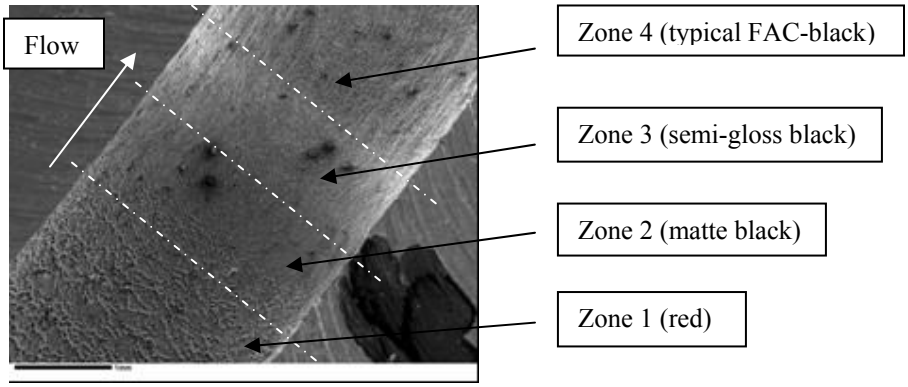

Fig.12 Oxide transition zone discovered in RUN-3

Probe radius data from the first part of RUN-3 reveals FAC rates of 2.6 mm/a and 0.8 mm/a for 1.6 mm and 2.4 mm probes, respectively. Also, mass transfer coefficients for these probes were estimated to be 6.6 mm/s and 3.5 mm/s for 1.6 mm and 2.4 mm probes, respectively [7]. These results are in good agreement with those found by Woolsey [8].

For the second part of RUN-3 with fresh probes, oxygen was injected step-wise and the oxygen stifling concentration was determined from the radius data as 1.2±0.4 ppb (see Figure 13)

It is important to note that the controlling mechanisms at elevated pH may be different because of the large difference in magnetite solubility between neutral and ammoniated chemistries and the probable difference in dissolution kinetics.

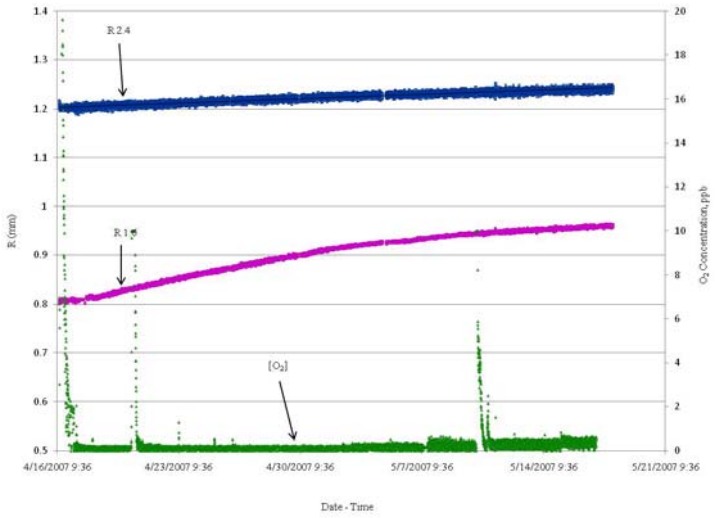

Fig.13 Probe radii – RUN-3, second part

3.5. RUN-4

For this run, pH was raised to ~10 by the addition of more ammonia and new probes were installed in the test sections. The oxygen concentration was maintained well below 1 ppb (see Figure 14), except for the initial oxygen spike (< 25ppb). No detectable corrosion was observed in this run. Since high pH can also help reducing the FAC rate, it is uncertain whether the high pH or $[O_2]$, or both, are responsible for the stifling in this run.

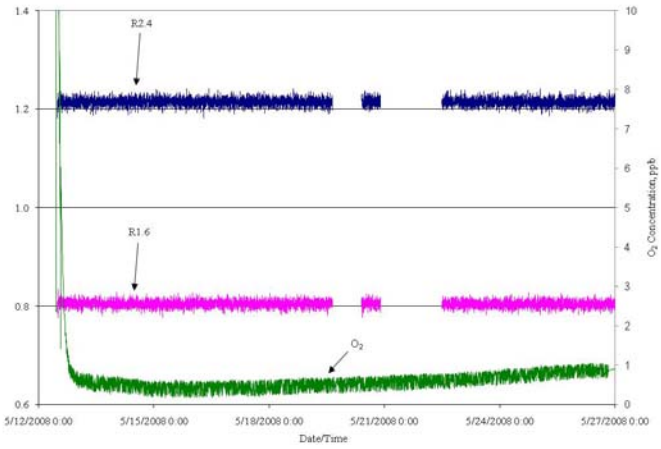

Fig.14 Probe radii – RUN-4

For all chemistry conditions investigated so far, the effect of oxygen undoubtedly is to interact with the oxide film on the probes surface. It is postulated for stifling to happen, oxygen has to diffuse through the pores of the magnetite in the oxide film to the oxide-metal interface, and the minimum oxygen concentration in the solution necessary to provide this driving force is essentially the threshold oxygen concentration value for stifling. This minimum oxygen concentration is just enough to react with the Fe^{2+} ions as they are produced. It should be noted that in diffusing through the oxide layer oxygen may also react with Fe^{2+} ions in the oxide surface and may never reach the metal if the driving force is too low. Conversely, when the coolant flowing over a surface which has already a protective passive film becomes depleted in oxygen, the oxide has to be reduced to some extent before the production of Fe^{2+} ions can recommence at the metal (by corrosion).

3.6. RUN-5

To reproduce plant conditions more closely and study representative FAC, the loop was dosed with hydrazine. The target chemistry for this run was $pH_{25^{\circ}C} \sim 9.2$ with NH_3, $[N_2H_4] = 100$ ppb. After adjusting and maintaining the chemistry at the desired condition for ~ 2 weeks (daily additions of N_2H_4 equivalent to 45 ppb were required), a new set of probes was installed and RUN-5 was commenced. At the time of writing, the run is still in progress. While there has not yet been detectable corrosion in the upstream 2.4 mm probe, the 1.6 mm probe has been corroding at the rate of ~2.5 mm/a. This is comparable with the FAC rate of ~2.9 mm/a of the 1.6 mm probe in RUN-3 which had a pH of 9.2 but no hydrazine.

4. Mechanisms behind FAC

According to these experimental results, it seems that the mechanisms behind FAC are different under different water chemistries. FAC rates at feedwater conditions have often been assumed to be mass-transfer controlled [9]. This originates from the hypothesis that the metal is protected by the magnetite oxide film which forms on the surface and that this oxide film attains a steady-state thickness as the result of the balance between the dissolution of the oxide at the interface with coolant undersaturated in Fe^{2+} and the formation of oxide by corrosion at the interface with the metal. The magnetite formation is by the precipitation of roughly half of the dissolved iron released at the metal surface; the other half diffuses through the oxide film and is transported to the bulk coolant. This leads to a basic equation for FAC rate, R, as:

$$R = \frac{\Delta C}{\frac{0.5}{k_d} + \frac{1}{h}} \qquad (1)$$

Where ΔC is the undersaturation in iron, k_d is the dissolution rate constant, and h is the mass transfer coefficient. If, according to the common postulate, mass transfer controls, the dissolution term will be negligible and equation 1 will simplify to:

$$R = h.\Delta C \qquad (2)$$

For coolant of constant conditions (very low or no dissolved iron content), ΔC approaches the solubility of the oxide (which is assumed constant under a specific chemistry) and thus, R varies as the mass transfer coefficient. Steels having oxides with different solubilities may experience different FAC rates (for example probes in RUN-1 with higher Cr content compared to those in RUN-2 with lower Cr content at zero oxygen condition). The dissolution rates (i.e. values of k_d) of the oxides may also be different. Thus, a more detailed analysis of the effects of flow under the different chemistry conditions of these runs in fact has suggested that simple mass transfer considerations are inadequate for describing FAC in high pH coolant [10][11].

5. Conclusions

FAC is a major phenomenon in the wall thinning of carbon steel piping in the secondary system of power plants. FAC is influenced by several parameters synergistically.

Different steels corrode at different rates. This is probably because oxide solubilities are different resulting in a different driving force for mass transfer at the interface with the coolant. The lower Cr content in the material used in RUN-2 compared with the one used in RUN-1 is probably responsible for a less protective oxide film and therefore higher FAC rates (under similar experimental conditions).

Oxygen dosing has been proved to be a very effective method of preventing FAC. With careful control of feed-water oxygen and hydrazine concentrations, it is possible to control FAC in feed systems. The threshold oxygen concentration for stifling FAC under neutral chemistry was about 40 ppb. At $pH_{25^\circ C}$ 9.2 with ammonia in RUN-2 and RUN-3 the threshold concentration was about 1.2 ppb. No detectable FAC was observed at $pH_{25^\circ C}$ 10 in RUN-4, the reason for which could be high pH chemistry or $[O_2]$ or both. So, it is not possible to determine a threshold oxygen concentration for stifling under this chemistry condition since pH effect might be predominant.

Stifling of FAC seemed to proceed along with an oxidation front that moves downstream. Higher $[O_2]$ upstream of this front deposits hematite on top of magnetite.

6. Acknowledgment

The authors' various organizations are thanked for supporting this research program.

7. References

[1] http://81.194.11.10/vf/05_inf/05_inf_1dossiers/05_inf_41_mihama/05_inf_41_mihama.shtm

[2] "Final Report about Mihama-3 Secondary System Piping Failure", Nuclear & Industrial Safety Agency, Tokyo, Japan, 2005

[3] Lister D.H. et al. "Fundamental Study of Flow-Accelerated Corrosion", *Report on Phase I*, 2005 – 2008.

[4] Tremaine P.R. and LeBlanc J.C., "The Solubility of Magnetite and the Hydrolysis and Oxidation of Fe^{2+} in Water to 300 ^{o}C", *J. Solution Chem.,* Vol. 9 No. 6 1980.

[5] Woolsey I.S, Bignold G.J, De Whalley C.H, and Garbett K, "The Influence of Oxygen and Hydrazine on the Erosion-Corrosion Behavior and Electrochemical Potentials of Carbon Steel under Boiler Feedwater Conditions", Proc. 4th BNES Internl. Conf. on Water Chem. of Nucl. Reactor Systems, Bournemouth, UK, 1986.

[6] Lister D.H[1], Feicht A[1], Cook W.G[1], Khatibi M[1], Liu L[1], Ohira T[2], Kadoi E[2], Takiguchi H[2], Fujiwara K[3], and Uchida S[4], "Effects of Dissolved Oxygen on Flow-Accelerated Corrosion in Feedwater Systems", 13th International Conference on Environmental Degradation of Materials in Nuclear Systems, Whistler, BC, 2007.

[7] Berger, F.P. and Hau, K-F. F-L., "Mass Transfer in Turbulent Pipe Flow Measured by the Electrochemical Method", *Internl. J. Heat and Mass Trans.*, 20, 1185, 1977.

[8] Woolsey, I.S., "Erosion-Corrosion in PWR Secondary Circuits", *CEGB Rept. TPRD/L/3114/R87*, 1987.

[9] Berge, P., Ducreux, J. and Saint-Paul, P., « Effects of Chemistry on Erosion Corrosion of Steels in Water and Wet Steam", Proc. 2nd. BNES Internl. Conf. on Water Chem. of Nucl. Reactor Systems, Bournemouth, UK, 1980.

[10] Lister, D.H. and Lang, L. "A Mechanistic Model for Predicting Flow-assisted and General Corrosion of Carbon Steel in Reactor Primary Coolants", Proceedings Water Chemistry, Avignon, France, 2002.

[11] D.H. Lister[1], W. Cook[1], A. Feicht[1], K. Fujiwara[2], E. Kadoi[3], M. Khatibi[1], L. Liu[1], T. Ohira[3], H. Takiguchi[3] and S. Uchida[4], "A Laboratory Study of Flow-Accelerated Corrosion in Feedwater Systems", 16th Pacific Basin Nuclear Conference (16PBNC), Aomori, Japan, 2008.